And., Intl.,J., Appl Sci., Eng., Tech, Vol 03, No 03, November 2023
e-ISSN: 2797-0442

Overcurrent and Directional Overcurrent Protection for Microgrid

Zahira Shiva Salsabila, Adrianti*, Muhammad Nasir
Department of Electrical Engineering, Universitas Andalas, Padang, Indonesia
*Corresponding author, e-mail: adrianti@eng.unand.ac.id

Abstract— Microgrids will become common in future distribution networks. Numerous operating modes that occur in microgrids make the development of protection schemes and settings challenging. This paper aims to develop a simple protection scheme for the Microgrid IEC Benchmark without any expensive equipment such as communication apparatus. The scheme consists of directional and non-directional overcurrent relays with standard inverse characteristics. For the simulation tool, Digsilent powerfactory is employed. Four operating modes of the microgrid are applied to verify the relays' coordination. The results show that the proposed scheme successfully protects the microgrid during short circuit faults with acceptable time margins.

Keywords: Overcurrent Protection, Microgrid, and Distributed Generation.

This article *is licensed under the CC–BY-SA license.*

1. Introduction

Microgrids have received lots of attention as local power supply and loads due to their efficient and resilient benefit [1]. The transformation into renewable energy sources has promoted distributed generations which is the beginning of microgrids. A microgrid consists of several distributed generations (DGs) and can operate while connected or disconnected to a grid. The DGs may supply or not supply the microgrid, at any given time for many reasons. Therefore, the magnitude and direction of electric current during normal and fault conditions vary greatly, which is very similar to transmission networks. The microgrid current variation results in complexity for the microgrid protection system, since most microgrid protections are current-based.

The paper aims to develop a simple protection scheme for a microgrid called Microgrid IEC Benchmark [2]. The protection scheme for the Microgrid IEC Benchmark has been proposed in [3] and [4]; however, they use overcurrent relays, which are considered less effective because they cannot differentiate the current directions. Current direction can be detected by a Directional Over Current Relay (DOCR), therefore this kind of relay is often applied in a network with DGs [5], [6]. In [7], the authors proposed overcurrent relays for earth fault protection of the Microgrid IEC Benchmark. Authors in [8] also proposed DOCR for the Microgrid IEC Benchmark. The DOCRs are tested with four mode operations i.e. (a) grid-connected to the microgrid without any DG, (b) grid-connected to the microgrid with all DGs operating, (c) grid-connected to the microgrid with DG1 and DG2 operating, (d) islanding operation of the microgrid with all DGs operating. While in this paper, the mode operations are mode (1) and (2) which is equivalent to mode (b) and (d) as in [8] and then mode (3): grid-connected to the microgrid with all DGs operating except DG1 and mode (4): grid-connected to the microgrid with all DGs operating except DG2. These operating modes are considered more reasonable since the probability of only one DG off at one time is higher than the probability of two DGs off or even all DGs off at a time.

Several papers proposed adaptive protection for distribution networks with DGs [9]–[12]. These adaptive protections are considered more powerful than non-adaptive ones. However, adaptive

Received: October 01, 2023, Revised: December 12, 2023, Accepted: December 14, 2023
https://doi.org/10.25077/aijaset.v3i3.103

protections need communication networks [9], [12], which considered do not cost effective for small capacity of DGs.

2. Methodology

The single line diagram of the Microgrid IEC Benchmark is shown in Figure 1. The microgrid consist of four group DGs i.e. DG1 and DG3 with synchronous generator, three inverter-faced wind generations as DG2 and six-unit DFIG wind generations as DG4. Data of the microgrid are available in [2].

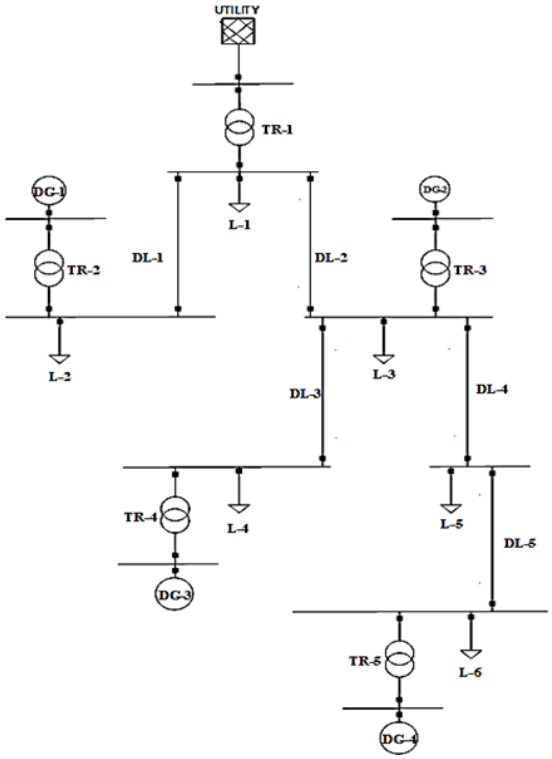


Figure 1. The Microgrid IEC Benchmark

The research methodology is depicted in the flowchart in figure 2. The setting of the relays in the microgrid have to coordinate well for the four operating modes as shown in Table 1. The simulations are carried out using Digsilent Powerfactory which consist of power flow, three phase short circuit and phase to phase short circuit simulation. Coordination among relays are assessed from current – time plot that generated for each relays.

Table 1. Operating mode of the Microgrid

Mode	Grid	DG1	DG2	DG3	DG4
1	on	on	on	on	on
2	off	on	on	on	on
3	on	off	on	on	on
4	on	on	off	on	on

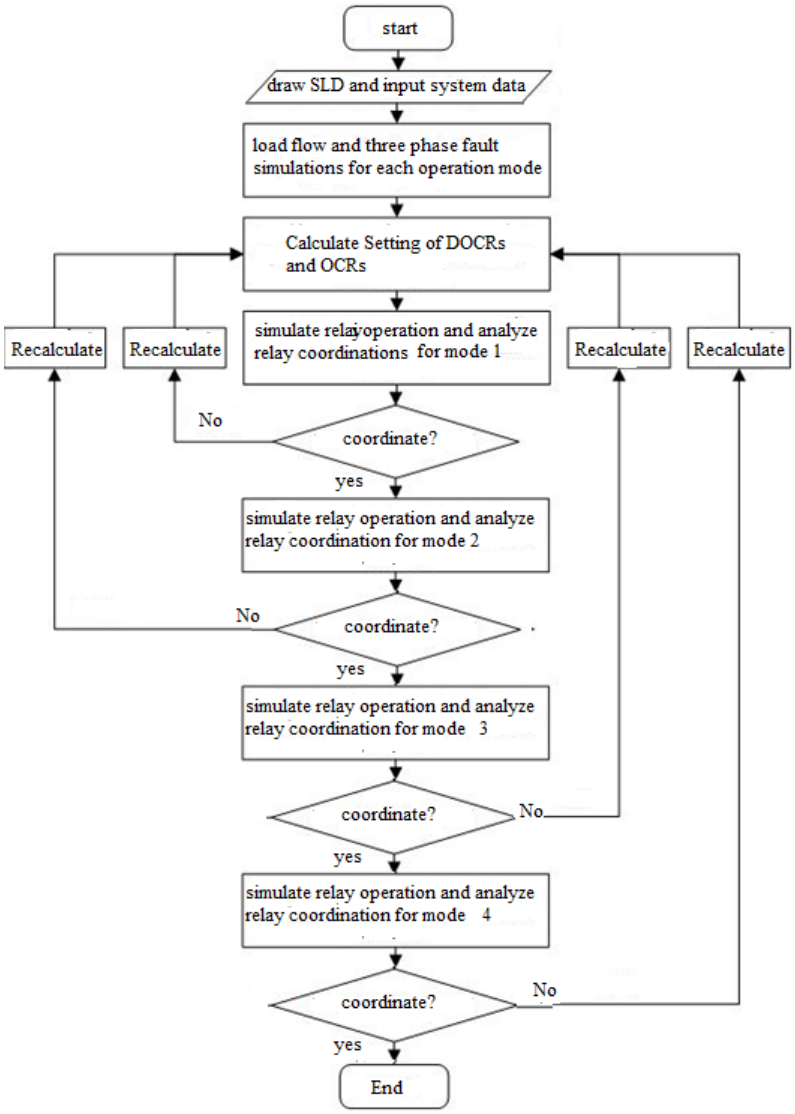


Figure 2. Flowchart of the research method

There are 15 relays are installed in the microgrid. Ten of them is DOCRs that installed on each end of the lines. Five other relays are OCR that installed on the point of common coupling (PCC) of the DGs and the microgrid. Pick up setting of the relays are calculated using equation (1) and (2)

$$I_{pickup-pri} = (1.1\sim1.2)I_{max} \tag{1}$$

$$I_{pickup-sec} = I_{pickup-pri} \times \frac{1}{CT\ ratio} \tag{2}$$

where I_{max} is the largest of normal current that flow on the relay.

The Standard Inverse characteristic is chosen for the relays except for the relay at the DG2 terminal, which uses definite time OCR, since an inverter faced wind generation supplies very limited fault current. Time setting of the standard inverse relays are calculated using equation (3) to (4).

$$PSM = \frac{I_f}{I_{pickup-pri}} \tag{3}$$

$$t_{op} = \frac{TMS \times 0.14}{PSM^{0.02} - 1} \quad (4)$$

Where I_f is the largest fault current seen by the relay, t_{op} is operating time of the relay and TMS is time multiplier setting.

3. Result and Discussion

Names and locations of the relays on the microgrid is shown in Figure 3. The distribution lines have rated voltage of 25 kV.

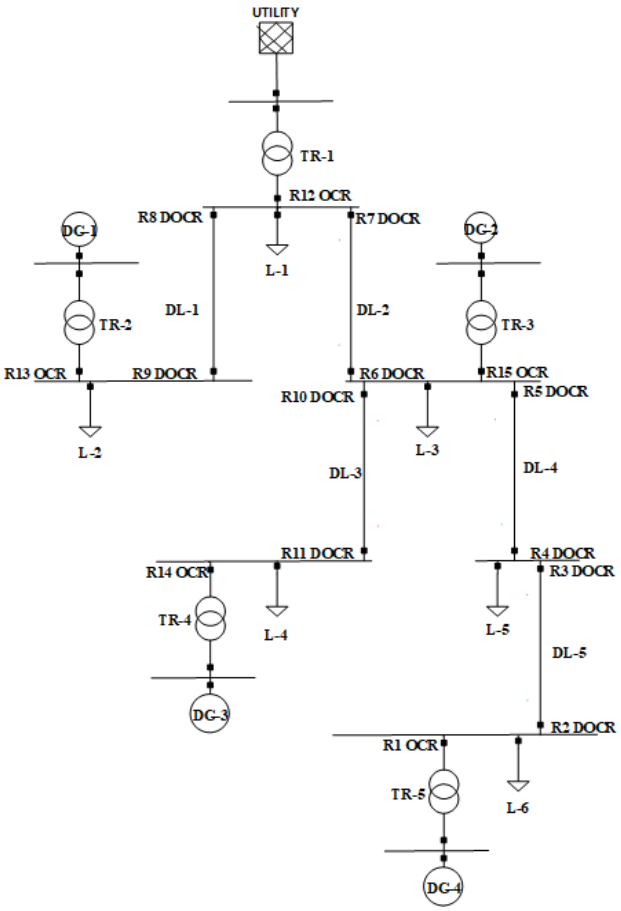


Figure 3. Relays of the protection scheme

The largest normal current that seen by the relays are obtained from powerflow simulation of different operating modes. The results are shown in Table 2 and will be used to calculate relay's pick-up settings.

Tabel 2. The largest normal currents seen by the relays

Relay-type	Imax (A)	Relay-type	Imax (A)	Relay-type	Imax (A)
R3 DOCR	73	R12 OCR	183	R11 DOCR	52
R5 DOCR	62	R6 DOCR	50	R9 DOCR	50
R10 DOCR	52	R4 DOCR	62	R13 OCR	170
R7 DOCR	58	R2 DOCR	73	R14 OCR	159
R8 DOCR	129	R1 OCR	149	R15 OCR	87

Time setting i.e. TMS of the relays are calculated based on operating time of the relays for the largest fault current. Therefore, three phase fault simulation of different operating modes are carried out in order to find the largest fault current seen by the relays. The results are shown in Table 3.

Table 3. Fault currents for TMS calculation

Relay	If (A)	Relay	If (A)	Relay	If (A)
R3	681	R12	8270	R11	502
R5	681	R6	879	R9	502
R10	1442	R4	379	R13	846
R7	1063	R2	553	R14	846
R8	8770	R1	1021	R15	35

Using Equation (1) to (4), setting of the relays are calculated. The relay settings, CT ratios and relay's directions are shown in Table 4.

Table 4. Setting of the relays

Relay	CT ratio	$I_{pickup-sec}$	TMS	Relay direction
R3	100:1	0,803	0,100	*Forward*
R5	100:1	0,682	0,242	*Forward*
R10	100:1	0,572	0,130	*Forward*
R7	100:1	0,638	0,382	*Forward*
R8	150:1	0,946	0,150	*Forward*
R6	100:1	0,55	0,130	*Reverse*
R4	100:1	0,682	0,179	*Reverse*
R2	100:1	0,803	0,277	*Reverse*
R11	100:1	0,572	0,259	*Reverse*
R9	100:1	0,55	0,296	*Reverse*
R1	200:1	0,8195	0,331	-
R12	250:1	0,8052	0,560	-
R13	200:1	0,935	0,271	-
R14	200:1	0,8745	0,264	-
R15 def-time	100:1	0,975	Time-set 0,400 s	-

Relay coordinations are checked using current-time plot that generated by Digsilent Powerfactory. For example, a fault on line DL4 will trigger R4 and R2 to disconnect fault current from downstream of the network as shown in Figure 4. R4 acts as the primary protection and operate faster (0.723 s) than R2 as the backup protection (1.209 s). The time margin between R4 and R2 is 0.486, hence the coordination is considered good.

AIJASET – Vol. 03, No. 03, November 2023. 179-187
https://doi.org/10.25077/aijaset.v3i3.103

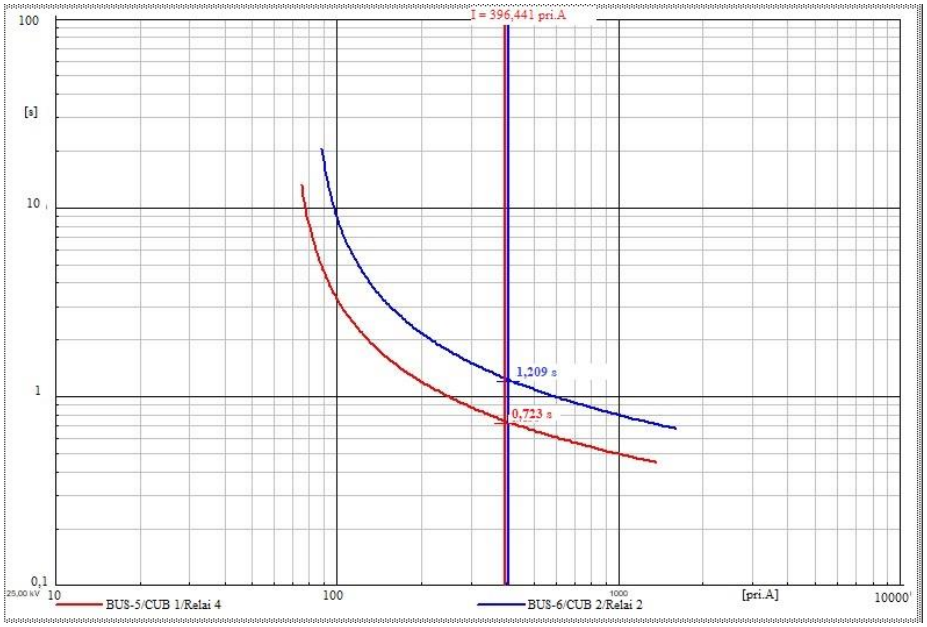


Figure 4. Current-Time plot of R4 and R2 for a fault on line DL4

The relay coordinations have been tested for faults on different location during different operating modes. The coordination results of three phase faults during operation mode 1 are shown in Table 5. The grading margin between relays are larger than 4 seconds, hence the relays' coordination are good. The relays are also tested for two phase faults during operation mode 1 which also give good relay coordinations.

Table 5. Relays' coordination for three phase faults during operation mode 1

Fault location	Relay's operating time (seconds)		
	Main	Back-Up	
50% DL5	R2 (0.941) →	R1 (1.738)	
	R3 (0.389) →	R5 (0.822) →	R11 (1.411)
		→	R7 (1.648)
50% DL4	R4 (0.723) →	R2 (1.209) →	R1 (2.321)
	R5 (0.642) →	R11 (1.010) →	R14 (2.245)
		R7 (1.183) →	R12 (3.780)
50% DL3	R10 (0.350) →	R7 (1.142) →	R12 (3.509)
		R4 (1.243) →	R2 (1.905)
	R11 (0.722) →	R14 (1.248)	
50% DL2	R6 (0.355) →	R11 (0.919) →	R14 (1.912)
		R4 (1.075) →	R2 (1.711)
	R7 (0.882) →	R12 (1.797)	
	→	R9 (1.899)	
50% DL 1	R9 (0.790) →	R13 (1.354)	
	R8 (0.423) →	R6 (1.117) →	R11 (2.657)
		R12 (1.779)	

Table 6 shows operating time of relays for three phase faults during operation mode 2. It can be seen that grading margin between relays are more than 4 seconds, hence the relays' coordination are good. The same simulation for two phase faults also give correct coordination among the relays.

Table 6. Relays' coordination for three phase faults during operation mode 2

Fault location	Relay's operating time (seconds)		
	Main	**Back-Up**	
50% DL5	R2 (0.936) →	R1 (1.617)	
	R3 (0.458) →	R5 (0.957) →	R11 (1.191)
		→	R9 (1.776)
			R7 (3.738)
50% DL4	R4 (0.718) →	R2 (1.197) →	R1 (2.281)
	R5 (0.767) →	R11 (0.950)→	R14 (2.008)
		R9 (1.324) →	R7 (2.111)
50% DL3	R10 (0.433) →	R4 (0.978) →	R2 (1.571)
		R9 (1.269) →	R7 (1.972)
	R11 (0.738) →	R14 (1.321)	
50% DL2	R6 (0.359) →	R11 (0.951) →	R14 (2.021)
		R4 (1.048) →	R2 (1.659)
	R9 (01.018) →	R7 (1.458) →	R13 (2.114)
50% DL1	R9 (0.831) →	R13 (1.485)	
	R6 (0.436) →	R8 (1.055)	
		R11 (1.542) →	R14 (3.030)
		R4 (1.894) →	R2 (2.424)

For operating mode 3 and 4, the relays' operating time is shown in Table 7 and 8 respectively. In these operating modes, the relays also provide correct coordination for three phase faults and for two phase faults.

Table 7. Relays' coordination for three phase faults during operation mode 3

Fault location	Relay's operating time (seconds)		
	Main	**Back-Up**	
50% DL5	R2 (0.941) →	R1 (1.631)	
	R3 (0.390) →	R5 (0.825) →	R11 (1.410)
		→	R7 (1.664)
50% DL4	R4 (0.723) →	R2 (1.280) →	R1 (2.320)
	R5 (0.644) →	R11 (1.011)→	R14 (2.248)
		R7 (1.191) →	R12 (2.992)
50% DL3	R10 (0.352) →	R7 (1.149) →	R12 (2.858)
		R4 (1.232) →	R2 (1.891)
	R11 (0.732) →	R14 (1.277)	
50% DL2	R6 (0.355) →	R11 (0.921) →	R14 (1.922)
		R4 (1.072) →	R2 (1.706)
	R7 (0.822) →	R12 (1.710)	
50% DL1	R6 (1.201) →	R11 (2.811)	
	R8 (0.422) →	R12 (1.733)	

Table 8. Relays' coordination for three phase faults during operation mode 4

Fault Location	Relay's operating time (seconds)		
	Main	Back-Up	
50% DL5	R2 (0.938) →	R1 (1.624)	
	R3 (0.397) →	R5 (0.837) →	R11 (1.441)
		→	R7 (1.560)
50% DL4	R4 (0.720) →	R2 (1.202) →	R1 (2.380)
	R5 (0.648) →	R11 (1.031)→	R14 (2.327)
		R7 (1.171) →	R12 (3.678)
		→	R9 (4.774)
50% DL3	R10 (0.352) →	R7 (1.137) →	R12 (3.464)
		R4 (1.223) →	R2 (1.875)
	R11 (0.731) →	R14 (1.299)	
50% DL2	R6 (0.416) →	R11 (0.933) →	R14 (1.956)
		R4 (1.051) →	R2 (1.669)
	R7 (0.822) →	R12 (1.797)	
		R9 (1.924)	
50% DL1	R9 (0.790) →	R13 (1.355)	
	R8 (0.423) →	R12 (1.763)	R6 (2.681)

4. Conclusion

The proposed protection scheme consists of ten DOCR for each end of the lines and 5 OCR for the DG terminals and the Grid. The relays have standard invers characteristics, except for DG2 terminal which has definite time characteristic. The calculated settings have been tested using Digsilent Powerfactory simulation and provide good coordination between relays for each operating mode, where the grading margin between relays is always greater than four seconds.

References

[1] M. W. Altaf, M. T. Arif, S. N. Islam, and M. E. Haque, 'Microgrid Protection Challenges and Mitigation Approaches–A Comprehensive Review', *IEEE Access*, vol. 10, pp. 38895–38922, 2022, doi: 10.1109/ACCESS.2022.3165011.

[2] S. Kar, 'A comprehensive protection scheme for micro-grid using fuzzy rule base approach', *Energy Systems*, vol. 8, no. 3, pp. 449–464, Aug. 2017, doi: 10.1007/s12667-016-0204-x.

[3] S. M. Saad, N. El-Naily, and F. A. Mohamed, 'A new constraint considering maximum PSM of industrial over-current relays to enhance the performance of the optimization techniques for microgrid protection schemes', *Sustainable Cities and Society*, vol. 44, pp. 445–457, Jan. 2019, doi: 10.1016/j.scs.2018.09.030.

[4] S. D. Saldarriaga-Zuluaga, J. M. López-Lezama, and N. Muñoz-Galeano, 'An Approach for Optimal Coordination of Over-Current Relays in Microgrids with Distributed Generation', *Electronics*, vol. 9, no. 10, 2020, doi: 10.3390/electronics9101740.

[5] A. Adrianti and N. Mukhlisiah, 'Rekonfigurasi Relai Proteksi setelah Penambahan Pembangkit Tersebar pada Jaringan Distribusi', *Jurnal Nasional Teknik Elektro*, pp. 84–89, 2017.

[6] Adrianti, A, Wahyuni, S, and Nasir, M, 'Overcurrent relay coordination with grid-connected and islanding capability on distribution network with distributed generation', presented at the IOP Conference Series: Materials Science and Engineering, IOP Publishing, 2019, p. 012002.

[7] N. El-Naily, S. M. Saad, and F. A. Mohamed, 'Novel approach for optimum coordination of overcurrent relays to enhance microgrid earth fault protection scheme', *Sustainable Cities and Society*, vol. 54, p. 102006, Mar. 2020, doi: 10.1016/j.scs.2019.102006.

[8] S. D. Saldarriaga-Zuluaga, J. M. López-Lezama, and N. Muñoz-Galeano, 'Optimal Coordination of Overcurrent Relays in Microgrids Considering a Non-Standard Characteristic', *Energies*, vol. 13, no. 4, 2020, doi: 10.3390/en13040922.

[9] D. Gutierrez-Rojas, P. H. J. Nardelli, G. Mendes, and P. Popovski, 'Review of the State of the Art on Adaptive Protection for Microgrids Based on Communications', *IEEE Transactions on Industrial Informatics*, vol. 17, no. 3, pp. 1539–1552, Mar. 2021, doi: 10.1109/TII.2020.3006845.

[10] P. H. A. Barra, D. V. Coury, and R. A. S. Fernandes, 'A survey on adaptive protection of microgrids and distribution systems with distributed generators', *Renewable and Sustainable Energy Reviews*, vol. 118, p. 109524, Feb. 2020, doi: 10.1016/j.rser.2019.109524.

[11] A. Ataee-Kachoee, H. Hashemi-Dezaki, and A. Ketabi, 'Optimized adaptive protection coordination of microgrids by dual-setting directional overcurrent relays considering different topologies based on limited independent relays' setting groups', *Electric Power Systems Research*, vol. 214, p. 108879, Jan. 2023, doi: 10.1016/j.epsr.2022.108879.

[12] M. S. Elbana, N. Abbasy, A. Meghed, and N. Shaker, 'μPMU-based smart adaptive protection scheme for microgrids', *Journal of Modern Power Systems and Clean Energy*, vol. 7, no. 4, pp. 887–898, Jul. 2019, doi: 10.1007/s40565-019-0533-6.